JOURNAL OF SOLID STATE CHEMISTRY 61, 359–368 (1986)

Neutron Diffraction Study of the Anion-Excess Fluorite-Related $Ca_{1-x}Th_xF_{2+2x}$ Solid Solution

J. P. LAVAL, A. MIKOU, AND B. FRIT*

Laboratoire de Chimie Minérale Structurale, L.A.-CNRS. n° 320, U.E.R. des Sciences, 123, Avenue Albert Thomas, 87060 Limoges, Cedex, France

AND J. PANNETIER

I.L.L., 156X, 38042 Grenoble, France

Received May 6, 1985

The defect structure of $Ca_{1-x}Th_xF_{2+2x}$ solid solution ($0 \leq x \leq 0.18$) has been examined by powder neutron diffraction. Two kinds of $\langle xxx \rangle$ interstitials whose respective numbers increase linearly with increasing dopant concentration, can be distinguished: one labeled F″ ($x \simeq 0.41$) is a true interstitial anion, the other noted F‴ ($x \simeq 0.30$) can be considered as a relaxed normal F anion. Two models of defect clusters, compatible with the observed distribution of F anions between normal and interstitial sites, and containing, respectively, one and two Th^{4+} cations, are proposed. In both clusters, Th^{4+} is 10-fold coordinated. Such clusters, which seem characteristic of large-size dopant cations, are suggested as possible defect-models for the $Pb_{1-x}Th_xF_{2+2x}$ solid solution.

Introduction

The defect properties of anion-excess fluorite-related solid solutions have been thoroughly investigated in recent years, by theoretical calculations based on computer simulation methods (*1–3*) and by various experimental techniques: thermal depolarization (*4, 5*), laser spectroscopy (*6–8*), dielectric relaxation and ionic conductivity (*9, 15*), EPR and Raman spectroscopy (*16, 17*), NMR (*18, 19*), and of course X-ray diffraction, Bragg, and diffuse neutron scattering (*20–31*).

For very low doping concentrations, isolated dopant cations and interstitial anions or simple dopant cation-interstitial anion pairs (nearest neighbor (nn) or next nearest neighbor (nnn) configurations), have been evidenced; however for moderate or high doping concentrations, there is now a general agreement about the presence in the structure of clusters associating one or several dopant cations, anionic vacancies and interstitial anions labelled X' at $\frac{1}{2},x,x$ site ($0.36 \leq x \leq 0.40$), X'' at x,x,x site ($x \simeq 0.40$), and X''' at x,x,x site ($0.28 \leq x \leq 0.30$) the latter being considered as relaxed normal X anions.

We have recently shown (*28*) that some of these clusters could be considered as precursors of the fully organized clusters present in ordered anion-excess fluorite-related superstructures, i.e., the discrete M_6X_{37} cluster consisting of an octahedral arrangement of six MX_8 square antiprisms

* To whom all correspondence is to be addressed.

0022-4596/86 $3.00

sharing corners to enclose a cuboctahedron of anions with an additional anion at its center (tveitite (*32, 33*), $Na_7Zr_6F_{31}$ (*34*) . . .) or the infinite monodimensional $(M_2X_8)_n$ cluster built up from double columns of isolated MX_8 square antiprisms, (Pb_3ZrF_{10} (*35, 36*)).

Despite these numerous results, a lot of experiments have still to be carried out in order to clearly understand the respective influence of factors like dopant cation concentration, dopant cation-to-anion size ratio, host cation polarizability, dopant cation size, and charge, on the structure of defect clusters. If we except the $Pb_{1-x}Th_xF_{2+2x}$ (*25*) and $Pb_{1-x}Zr_xF_{2+2x}$ (*27*) solid solutions, both characterized by a large number of F'''-type interstitials for low concentrations of M^{4+} cations and the $Na_{0.5-x}Y_{0.5+x}F_{2+2x}$ phase (*22*), all the previous Bragg scattering studies have been devoted to $M^{II}_{1-x}M^{III}_xF_{2+x}$ solid solutions. In order to investigate the role of dopant cation charge on defect clustering, we decided to study by neutron powder diffraction techniques the average structure of some disordered tetravalent cation-doped fluorites. As the localization of interstitial anions is obviously easier and more precise in small-size fluorite unit-cells containing cations of nearly the same size, we thought it was advisable to start this study with the $Ca_{1-x}Th_xF_{2+2x}$ solid solution.

Experimental

Intimate mixtures of calcium and thorium fluorides were heated at 950°C for 2 days in sealed platinum tubes. CaF_2 was a commercial product of 99.9% purity, carefully dried before use; ThF_4 was prepared by dehydratation at 750°C under anhydrous HF of high-purity $ThF_4 \cdot H_2O$. After reaction the platinum tubes were quenched in cold water. Powder X-ray photographs indicated the presence of a single face-centered cubic phase in each of the samples with $0 \leq x \leq 0.185$. Experiments performed at higher temperatures (maximum 1100°C) did not reveal any extension of the composition range. So, the upper limit value, $x = 0.24$ at 1500°C, previously proposed by Zintl and Udgard (*37*), is without any doubt overestimated, surely as a consequence of an insufficient protection of the samples against hydrolysis. The unit-cell parameter, obtained by least-squares refinement from accurate Guinier–Hägg data (silicon internal standard, $a_0 = 5.43088$ Å), increases linearly with increasing substitution rate x (Fig. 1) up to the maximum value $a_F = 5.596(3)$ for $x = 0.185$. Density measurements clearly indicate the nonstoichiometry to be compensated by excess anions.

Samples for powder neutron diffraction experiments were prepared at 950°C in sealed nickel tubes. The mixtures were first fired at 1000°C for 2 days, then ground fired again for 2 days at 950°C, and finally water-quenched. No attack of the tube by the fluorides was observed and the values of the cubic lattice parameter are exactly the same as for the experiments carried out in platinum tubes. Intensities at room temperature were collected at the Institut Laue-Langevin in Grenoble.

—On the D1A diffractometer, for $x = 0.075$, 0.125, and 0.150 samples (vanadium can, $\lambda = 1.384$ Å, exposure time: 10 hr for each).

—On the D1B diffractometer for $x = 0.10$

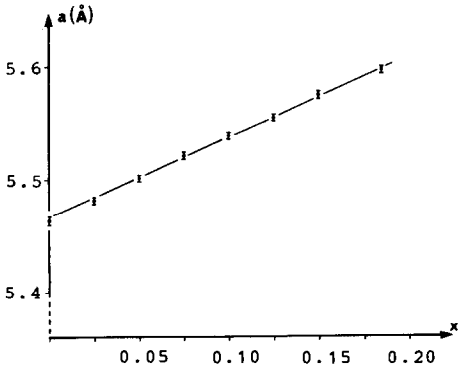

FIG. 1. Evolution with composition of the unit-cell parameter a_F of the $Ca_{1-x}Th_xF_{2+2x}$ solid solution.

and $x = 0.18$ samples (vanadium can, $\lambda = 1.282$ Å, exposure times: 2 × 2 hr for $x = 0.10$, 2 × 4 hr for $x = 0.18$). Bragg peaks were observed up to the (553) reflection. Their intensities listed on Table II were obtained by fitting the experimental profile to Gaussians and the background to a first-order polynomial; standard deviations were determined from the counting statistics. The diffraction pattern of the $x = 0.15$ sample is shown in Fig. 2. Observed (I_o) and calculated (I_c) intensities were adjusted by least-squares refinements to give structural parameters defining the contents of the average unit-cell. All structure refinement were performed in space group *Fm3m* using neutron scattering lengths of 4.90, 9.84, and 5.65 *Fm* for Ca, Th, and F, respectively. Overlapping data (e.g., 333 and 511 reflections) were included in each of the refinements (maximum 18 peaks analyzed). In order to localize interstitial fluorine atoms, difference Fourier sections based on initial refinements of the perfect fluorite lattice were calculated for every composition. One such section calculated in the (110) plane passing through the normal lattice anion, octahedral interstitial and cation sites, is shown on Fig. 3.

Results

No cation shift from ideal site (0,0,0) is observed and two interstitial positions are detected on the difference Fourier maps:

—the first labeled F″, at (x,x,x) with $x \simeq 0.41$ is a true interstitial position;

—the second labeled F‴, at (x,x,x) with $x \simeq 0.30$ actually corresponds to relaxed normal anions.

Full matrix least-squares refinements were performed on these bases, allowing

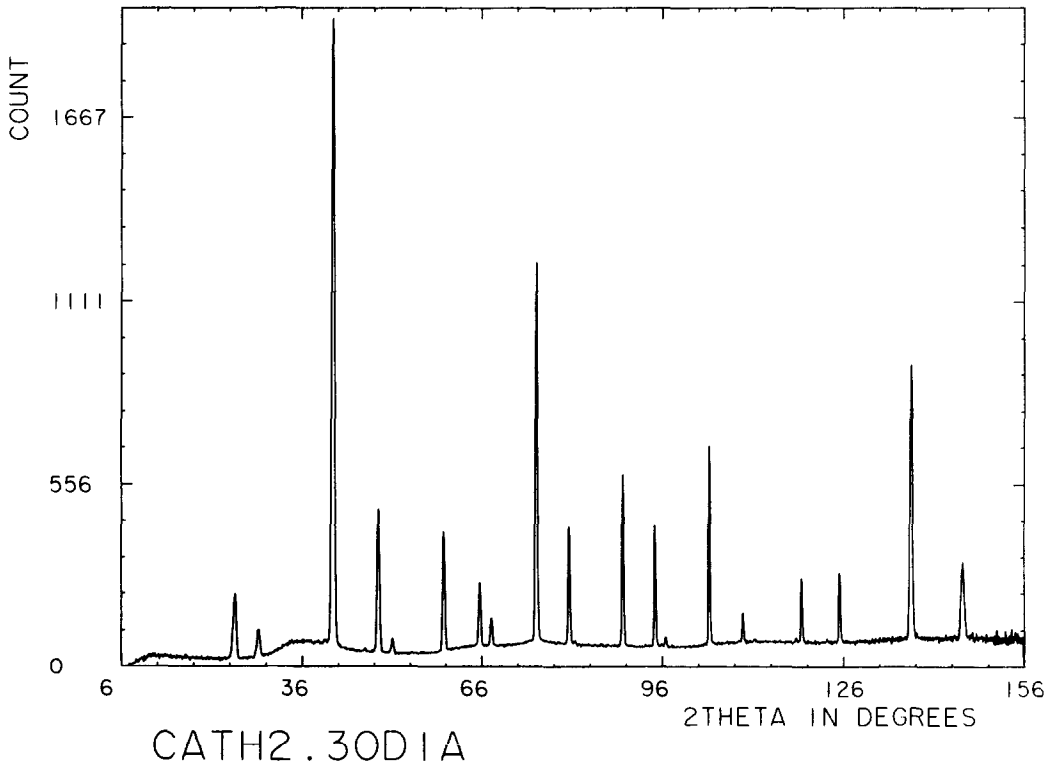

FIG. 2. Diffraction pattern of polycrystalline $(Ca,Th)F_{2.30}$ at room temperature (D1A diffractometer).

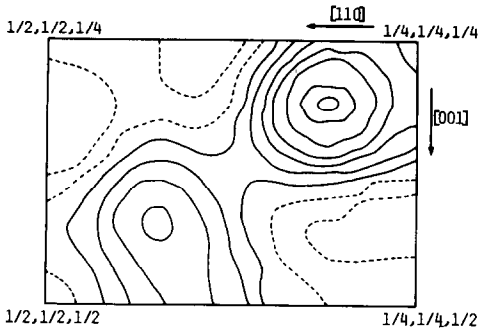

FIG. 3. Difference Fourier section in the (110) plane for the $(Ca,Th)F_{2.30}$ sample. Positive contours are shown as full lines and negative ones as broken lines.

simultaneously the cations and anions isotropic thermal coefficients, the anions coordinates and occupation numbers to vary. All the refinements converged quite well and led to very low R-values ($\lesssim 1\%$) and to very reasonable occupation rates ($n_F + n_{F''} + n_{F'''} \simeq 2 + 2x$). However, because of the closeness of the F''' and F sites, high correlations occurred between the parameters of these two sites and thus, it was difficult to obtain detailed and significant informations about the F''' interstitials. Refinements were then performed, allowing some parameters to vary, the others being held fixed at reasonable values. Whatever the refinement process, no change was observed for atom coordinates, for F'' interstitials occupancies and for the evolution with composition of anion occupancies. During the last cycles of refinement the sum of anion occupation numbers was constrained to be equal to $(2 + 2x)$. The best fit, with no large correlation coefficient, was obtained when the thermal parameters of F''' interstitials were fixed at the reasonable values listed on Table I; therefore we conclude that the structural parameters listed on this table provide the best description of the $Ca_{1-x}Th_xF_{2+2x}$ defect structure.

The evolution with x of the occupation numbers for normal F and interstitial F'' and F''' anions are shown on Fig. 4. Each evolution is linear and from the slopes of

TABLE I

FINAL VALUES OF REFINED PARAMETERS FOR THE $Ca_{1-x}Th_xF_{2+2x}$ SOLID SOLUTION

$2 + 2x$	2.15	2.20	2.25	2.30	2.36
a_F (Å)	5.521(3)	5.538(3)	5.555(3)	5.574(3)	5.594(3)
B_{Ca-Th} (Å^2)	0.96(2)	0.97(5)	1.07(2)	1.15(3)	1.35(6)
n_F	1.74(2)	1.68(6)	1.62(2)	1.52(2)	1.48(3)
B_F (Å^2)	1.24(2)	1.37(8)	1.62(2)	1.75(3)	1.65(7)
$x_{F''}$	0.413(2)	0.413(2)	0.412(1)	0.412(1)	0.410(1)
$n_{F''}$	0.21(2)	0.28(3)	0.35(2)	0.44(2)	0.50(2)
$B_{F''}$ (Å^2)	1.6(3)	2.1(6)	1.7(2)	1.8(2)	2.6(4)
$x_{F'''}$	0.298(2)	0.299(5)	0.302(2)	0.302(2)	0.306(2)
$n_{F'''}$	0.20(2)	0.24(6)	0.28(2)	0.34(2)	0.38(2)
$B_{F'''}$ (Å^2)	0.6	0.9	1.0	1.1	1.2
$R(I)\%$[a]	0.8	1.6	1.0	1.4	1.8
Instrument	D1A (10 H)	D1B (2 × 2 H)[b]	D1A (10 H)	D1A (10 H)	D1B (2 × 4 H)[b]

Note. The e.s.d. are given in parentheses and refer to the last digit.

[a] R is given as $\dfrac{\Sigma|I_o - I_c|}{\Sigma I_o}$.

[b] Higher e.s.d. for $MX_{2.20}$ and $M_{2.36}$ samples are a consequence of lower exposure time on D1B diffractometer.

TABLE II

EXPERIMENTAL (I_o) AND CALCULATED (I_c) INTENSITIES FOR THE $Ca_{1-x}Th_xF_{2+2x}$ SOLID SOLUTION

	$MF_{2.15}$		$MF_{2.20}$		$MF_{2.25}$		$MF_{2.30}$		$MF_{2.36}$	
h k l	I_o	I_c	I_o	I_c	I_o	I_c	I_o	I_c	I_o	I_c
1 1 1	18615	19499	18779	19000	19299	19006	17940	18375	18777	18731
2 0 0	12138	13651	10163	11413	8867	9438	6810	7110	6376	6223
2 2 0	136544	135099	137495	137640	142544	142951	146580	148725	153561	152633
3 1 1	21165	21811	23482	23433	26699	26911	30330	30180	31795	32956
2 2 2	5457	5627	4024	4665	3358	3765	2610	2925	2130	2664
4 0 0	26537	26673	25329	25486	24548	24156	23235	22935	21625	22072
3 3 1	10166	10455	10765	10885	11149	11600	11835	12360	11154	11715
4 2 0	9367	9350	7570	7507	5852	5993	5025	4770	4088	4198
4 2 2	70907	70737	68489	66572	66357	65526	64380	63645	62521	61660
5 1 1 / 3 3 3	12920	12903	14035	13741	16675	16773	18915	19380	19266	18680
4 4 0	26809	26741	24181	24464	25020	25232	25200	24945	23753	23621
5 3 1	13294	13141	13011	13328	15240	15289	16875	16500	15781	15662
6 2 0	36210	36057	30303	30493	28737	28835	25515	25785	23329	23103
5 3 3	3689	3655	3281	3378	3651	3586	3735	3480	2936	2512
4 4 4	11220	11475	8807	9109	9095	9421	8310	8595	7249	7339
5 5 1 / 7 1 1	8840	9061	7700	7853	9731	9788	10050	10185	8457	7402
6 4 2	75429	75446	—	—	62266	61973	57000	56940	40820	40872
7 3 1 / 5 5 3	19771	19618	—	—	20848	20685	21165	21225	—	—

the three curves we can propose the following evolution rates

$$\frac{2 - n_F}{x} = \frac{n_{V_F}}{n_{Th^{4+}}} \simeq 3, \frac{n_{F''}}{n_{Th^{4+}}} \simeq 3, \frac{n_{F'''}}{n_{Th^{4+}}} \simeq 2.$$

Then the substitutional mechanism can be written

$$Ca + 2F \rightarrow Th + 3F'' + 2F''' + 3V_F.$$

On the other hand, if we consider that F''' interstitials are not true interstitial anions, but only relaxed normal fluoride anions, then the number of true vacancies per Th^{4+} is $n_{V_F}/n_{Th^{4+}} = 1$, which gives the mechanism

$$Ca \rightarrow Th + 3F'' + V_F.$$

Cluster Models

All the anion-excess samples exhibit a modulated background (i.e., a diffuse scattering, increasing with increasing x values and centered mainly around $2\theta \simeq 36°$, just before the (220) peak; see Fig. 2) presum-

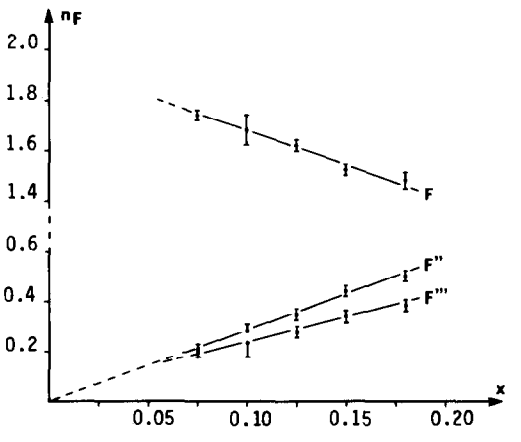

FIG. 4. Evolution with composition of the occupancies of normal F, and interstitial F'' and F''' anions.

ably arising from interaction between defects, i.e., from short-range order effects. As the currently known cluster models have all been proposed for solid solutions with mainly F′ or F′ and F″ interstitials, we had to devise an original model for our F″-containing solid solution.

An interesting feature of F″-based defect clusters is that, on the contrary of F′-based ones, there are no steric impossibilities for direct contact between F″ interstitials and normal F anions: in an average CaF_2/Th^{4+} fluorite cell with a mean $a_F = 5.55$ Å parameter, the shortest F–F″ distance is 2.27 Å, a value quite acceptable if we consider, first that the normal F atoms are probably slightly relaxed from their ideal fluorite positions, second that short F–F distances of this order occur in some ordered structures (2.22 Å in $PbZr_6F_{22}O_2$ (*39*) and 2.24 Å in $Na_7Zr_6F_{31}$ (*34*)). Thus the interpretation of the observed defect structure parameters of the $Ca_{1-x}Th_xF_{2+2x}$ solid solution does not require large-size clusters like the 4:4:3, or the "relaxed" 6:8:2 and 8:12:2 or the highly structured M_6X_{12} ones, proposed, respectively, for the $Ca_{1-x}Y_xF_{2+x}$ (*28*), $Pb_{1-x}Zr_xF_{2+2x}$ (*27*), and $Sr_{1-x}La_xCl_{2+x}$ (*30*) solid solutions.

The simplest cluster model assuming correct interanionic distances and regular cation coordinations is shown in Fig. 5. It associates, in the neighborhood of a dopant Th^{4+} cation, three F″ interstitials symmetrically distributed (threefold symmetry) around a normal fluorine vacancy V_F. Each original ThF_8 cube is then transformed into a regular ThF_{10} polyhedron, by substituting a triangular face for one corner. As a consequence of this substitution, a large number of short (2.27 Å) F–F″ distances are generated and one can expect the corresponding F atoms to be relaxed from their ideal fluorite positions. However, these atoms are not all in the same situation: some of them, like the atom noted F_1 in Fig. 5, are symmetrically surrounded, in addition to the five normal F atoms, by two F″ interstitials,

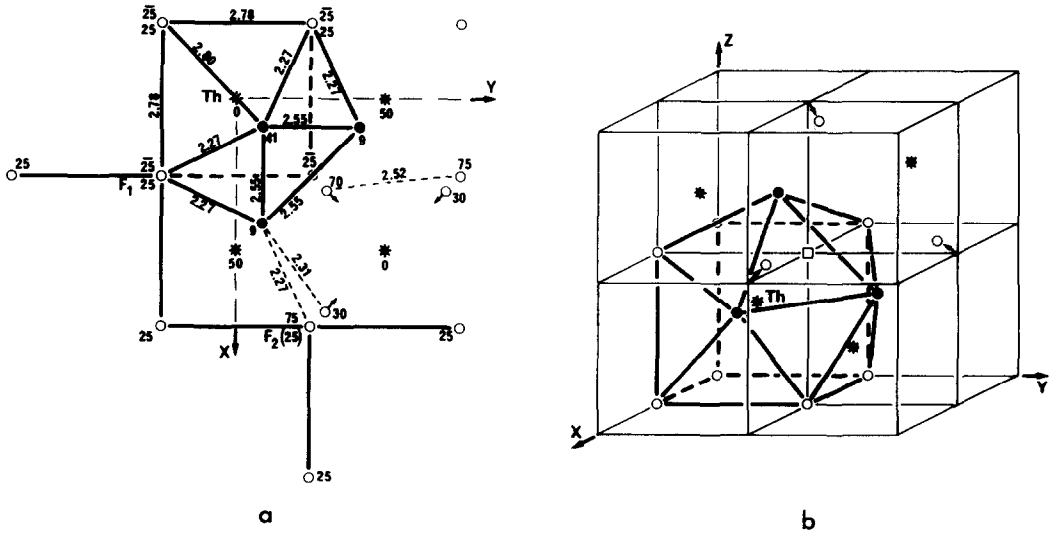

FIG. 5. Projection onto the (100)-fluorite plane (a) and spatial view (b) of the defect cluster associating around a Th atom, one normal fluorine vacancy V_F (at $z = 25$), three interstitials F″, and three relaxed anions F‴. Coordinates are given in $a/100$ units and anion–anion distances calculated for the $(Ca,Th)F_{2.25}$ sample are given in Ångstroms. (*) Cations (Ca,Th); (○) normal F anions; (□) normal fluorine vacancies V_F; (●) F″ interstitials; (○→, →○) F‴ relaxed anions.

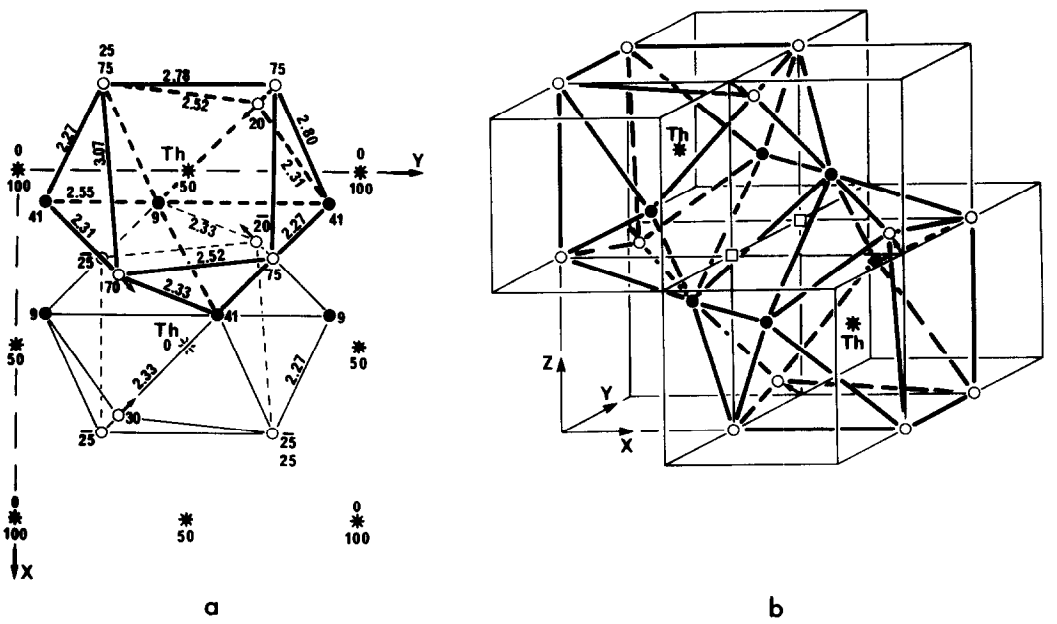

FIG. 6. Projection onto the (100)-fluorite plane (a) and spatial view (b) of the defect cluster associating two Th atoms, two normal fluorine vacancies V_F (at z = 25), six F″ interstitials, and four F‴ relaxed anions (same symbols and notation as in Fig. 5).

whereas others, like the atom noted F_2 in Fig. 5, have a dissymmetrical environment of five normal F atoms and only one F″ interstitial. Logically only the latter are actually relaxed. They are three and the directions of their shifts are illustrated by the small arrows of Fig. 5. As short anion–anion distances are a constant feature of this kind of phases, ordered or not, the F″–F‴ distances are only slightly increased (2.27 → 2.31 Å) by this local rearrangement, but the anionic network is now more regular. Each ThF_{10} polyhedron is surrounded by nine perfect or slightly distorted CaF_8 cubes and three hybrid CaF_9 polyhedra. The cation-to-anion distances, quite reasonable, are as follows: (Th,Ca)–F = 2.41 Å, (Th,Ca)–F″ = 2.39 Å, and Ca–F‴ = 2.29 Å.

Such a cluster, attractive as it may be, cannot however describe completely the $Ca_{1-x}Th_xF_{2+2x}$ solid solution at least for the high doping concentrations, since the number of F‴ relaxed anions per dopant cation Th^{4+} that it generates (3 F‴/Th^{4+}) is higher than the experimental one (2 F‴/Th^{4+}). This difficulty can be overcome by introducing the more sophisticated, but still very simple cluster, represented in Fig. 6. It is built up from two identical and almost regular ThF_{10} polyhedra sharing one edge, and associates on both sides of two nearest neighbor V_F vacancies, 6 F″ interstitials and two Th^{4+} dopant cations. The number of relaxed anions F‴ per dopant cation Th^{4+} is now exactly equal to the experimental value of 2.

It is difficult to choose definitively between these two models and further experiments like diffuse scattering would be of interest to determine the number of Th^{4+} present in defect clusters. It is quite likely however (as suggested by the slight nonlinearity of the $n_{F''} = f(x)$ curve for low substitutional rates ($x < 0.10$)) that both clusters are present in the solid solution, the simplest one, predominant for low doping con-

centrations, being progressively replaced by the largest one.

Comparison with the PbF_2/ThF_4 Solid Solution

From powder neutron diffraction study of the $Pb_{1-x}Th_xF_{2+2x}$ solid solution, Soubeyroux *et al.* (*25*) have shown that the interstitial fluorine atoms are distributed among three different positions (F′ at $\frac{1}{2},x,x$; $x \simeq 0.41$, F″ at x,x,x; $x \simeq 0.40$, and F‴ at x,x,x; $x \simeq 0.30$), whose occupancies are listed on Table III.

If we consider, first that only F′ and F″ atoms are true interstitials, F‴ atoms being relaxed normal F atoms, secondly that the F′ position is not very well defined and appears on published (*25*) difference Fourier sections essentially as the limit of a nonspherical F″ expansion, then the numbers of true vacancies $n_{V_F} = 2 - (n_F + n_{F'''})$ and true interstitials $n_{F_i} = n_{F'} + n_{F''}$, per dopant cation are, at least for the highly doped samples ($x > 0.10$), exactly the same as for the CaF_2/ThF_4 solid solution, i.e., $n_{V_F}/Th^{4+} = 1$, $n_{F_i}/Th^{4+} = 3$. Therefore, the same clusters could be present in both solid solutions, each Th^{4+} cation being at the center of a 10-fold coordination polyhedron more suited to its large size than the square antiprism suggested by Soubeyroux *et al.* However, close examination of the values listed in Table III, shows clearly that in the PbF_2/ThF_4 solid solution, the number of F‴ relaxed anions does not change with composition in the way it does in the CaF_2/ThF_4 one: instead of increasing linearly, it first increases superlinearly and then remains nearly constant. A quasisimilar evolution was observed for the $Pb_{1-x}Zr_xF_{2+2x}$ solid solution and we suggested (*27*) that this results from the linear aggregation of basic 4:4:2 clusters, leading to columnar complex clusters at the two ends of which relaxed anions were concentrated. It is not impossible that such a linear aggregation of the 2 Th^{4+} containing clusters (Fig. 6) through the F–F‴ edges, occurs in the $Pb_{1-x}Th_xF_{2+2x}$ solid solution. The presence in both solid solutions of the same chains of anionic vacancies, interstitial and relaxed anions, could then justify the analogy of their electrical properties. It is noteworthy that the evolution of ionic conductivity with composition in the $Pb_{1-x}In_xF_{2+x}$ solid solution (*42*) can also be interpreted by the formation of columnar clusters built up from sevenfold coordination polyhedra and isolated in the ordered Pb_2InF_7 structure (*36, 43*).

Conclusions

The unusual feature of the $Ca_{1-x}Th_xF_{2+2x}$ solid solution is the presence of F″ intersti-

TABLE III

ANION OCCUPANCIES FOR THE $Pb_{1-x}Th_xF_{2+2x}$ SOLID SOLUTION[a]

$2 + 2x$	2.05	2.10	2.20	2.25	2.30	2.40	2.46
n_F	1.98(1)	1.61(8)	1.50(8)	1.45(8)	1.45(10)	1.38(10)	1.46(10)
$n_{F'}$	0.07(1)	—	0.14(4)	0.18(3)	0.19(3)	0.28(3)	0.28(5)
$n_{F''}$	—	0.12(2)	0.19(4)	0.22(3)	0.25(3)	0.34(3)	0.41(5)
$n_{F'+F''}/x$	2.8	2.4	3.3	3.2	2.9	3.1	3.0
$n_{F'''}$	—	0.37(8)	0.37(8)	0.40(8)	0.41(10)	0.40(10)	0.31(10)
n_{V_F}/x^b	0.8	0.4	1.3	1.2	0.9	1.1	1.0

[a] Soubeyroux *et al.* (*25*).

[b] $n_{V_F} = 2 - (n_F + n_{F'''})$.

tials only. Differences with others M^{4+} doped fluorites clearly indicate that, if the dopant cation charge is not to be neglected since it controls, for obvious electrical neutrality conditions, the number of true interstitials per dopant cation, its size is the dominant factor in short-range order construction. As from a geometrical point of view, F′ interstitials are rather favorable to the formation of seven- or eightfold coordination polyhedra (square antiprisms, for instance), and F″ interstitials rather favorable to the formation of nine- or tenfold coordination polyhedra, we can expect, for CaF_2-based solid solutions the former to be predominant with small-size dopant cations (Zr^{4+}, heavy rare-earth cations, . . .) whereas the latter would be predominant with larger size dopant (U^{4+}, Th^{4+}, light rare-earth cations). This seems to be true for rare-earth cations since the ⟨111⟩ interstitial (F″) is a much more pronounced feature in La- than in Y-doped CaF_2 (*28, 29*), but many experiments are still to be carried out to check this hypothesis. Further experiments designed to investigate the effect of the host cation size (Ca < Sr < Pb < Ba) on the defect structure around a given dopant cation would also be valuable.

Acknowledgment

We are grateful to Professor B. T. M. Willis for several useful discussions.

References

1. C. R. A. Catlow, *J. Phys. C* **6,** 64 (1973).
2. J. Corish, C. R. A. Catlow, P. W. M. Jacobs, and S. H. Ong, *Phys. Rev. B: Condens. Matter* **25,** 6425 (1982).
3. R. J. Kimble Jr, P. J. Welcher, J. J. Fontanella, M. C. Wintersgill, and C. G. Andeen, *J. Phys. C* **15,** 3441 (1982).
4. S. H. Ong and P. W. M. Jacobs, *J. Solid State Chem.* **32,** 193 (1980).
5. E. Laredo, M. Puma, and D. R. Figueroa, *Phys. Rev. B: Condens. Matter* **19**(4), 2224 (1979).
6. D. S. Moore and J. C. Wright, *J. Chem. Phys.* **74**(3), 1626 (1981).
7. M. B. Seelbinder and J. C. Wright, *J. Chem. Phys.* **75**(10), 5070 (1981).
8. R. H. Petit, P. Evesque, and J. Duran, *J. Phys. C* **14,** 5081 (1981).
9. C. G. Andeen, J. J. Fontanella, M. C. Wintersgill, P. J. Welcher, R. J. Kimble Jr., and G. E. Matthews, Jr., *J. Phys. C* **14,** 3557 (1981).
10. J. Meuldijk, R. van der Meulen, and H. W. den Hartog, *Phys. Rev. B: Condens. Matter* **29**(4), 2153 (1984).
11. P. P. Fedorov, T. M. Turkina, B. P. Sobolev, E. Mariani, and M. Svantner, *Solid State Ionics* **6,** 331 (1982).
12. J. Schoonman, *Solid State Ionics* **5,** 71 (1981).
13. J. A. Archer, A. V. Chadwick, I. R. Jack, and B. Zeqiri, *Solid State Ionics* **9–10,** 505 (1983).
14. M. Ouwerkerk, E. M. Kelder, J. Schoonman, and J. C. van Miltenburg, *Solid State Ionics* **9–10,** 531 (1983).
15. J. M. Reau, S. Matar, G. Villeneuve, and J. L. Soubeyroux, *Solid State Ionics* **9–10,** 563 (1983).
16. D. J. Oostra and H. W. den Hartog, *Phys. Rev. B: Condens. Matter* **29**(5), 2423 (1984).
17. H. W. den Hartog and R. Nakata, *J. Phys. Soc. Jpn.* **52**(9), 3110 (1983).
18. R. J. Booth and B. R. McGarvey, *Phys. Rev. B: Condens. Matter* **21**(4), 1627 (1980).
19. S. H. N. Wei and D. C. Ailion, *Phys. Rev. B: Condens. Matter* **19**(9), 4470 (1979).
20. B. T. M. Willis, *Proc. Br. Ceram. Soc.* **1,** 9 (1964).
21. N. H. Anderson, K. Clausen, and J. K. Kjems, *Solid State Ionics* **9–10,** 543 (1983).
22. L. Pontonnier, G. Patrat, S. Aleonard, J. J. Capponi, M. Brunel, and F. de Bergevin, *Solid State Ionics* **9–10,** 549 (1983).
23. A. K. Cheetham, B. E. F. Fender, B. Steele, R. I. Taylor, and B. T. M. Willis, *Solid State Commun.* **8,** 171 (1970).
24. A. K. Cheetham, B. E. F. Fender, and M. J. Cooper, *J. Phys. C: Solid State Phys.* **4,** 3107 (1971).
25. J. L. Soubeyroux, J. M. Reau, S. Matar, C. Lucat, and P. Hagenmuller, *Solid State Ionics* **2,** 215 (1981).
26. C. Lucat, J. Portier, J. M. Reau, P. Hagenmuller, and J. L. Soubeyroux, *J. Solid State Chem.* **32,** 279 (1980).
27. J. P. Laval, C. Depierrefixe, B. Frit, and G. Roult, *J. Solid State Chem.* **54,** 260 (1984).

28. J. P. LAVAL AND B. FRIT, *J. Solid State Chem.* **49,** 237 (1983).
29. C. R. A. CATLOW, A. V. CHADWICK, AND J. CORISH, *J. Solid State Chem.* **48,** 65 (1983).
30. P. J. BENDALL, C. R. A. CATLOW, AND B. E. F. FENDER, *J. Phys. C* **17**(5), 797 (1984).
31. V. B. ALEXANDROV AND L. S. GARASHINA, *Dokl. Akad. Nauk. SSSR* **189,** 307 (1969).
32. D. J. M. BEVAN, O. GREIS, AND J. STRÄHLE, *Acta Crystallogr. Sect. A* **36,** 889 (1980).
33. D. J. M. BEVAN, J. STRÄHLE, AND O. GREIS, *J. Solid State Chem.* **44,** 75 (1982).
34. J. H. BURNS, R. D. ELLISON, AND H. A. LEVY, *Acta Crystallogr. Sect. B* **24,** 230 (1968).
35. J. P. LAVAL AND B. FRIT, *Mater. Res. Bull.* **14,** 1517 (1979).
36. B. FRIT AND J. P. LAVAL, *J. Solid State Chem.* **39,** 85 (1981).
37. E. ZINTL AND A. UDGARD, *Z. Anorg. Allg. Chem.* **240,** 150 (1939).
38. H. L'HELGOUALCH, G. FONTENEAU, AND J. PANNETIER, "Maryse," unpublished computer program, Univ. Rennes (1975).
39. J. P. LAVAL AND B. FRIT, *Rev. Chim. Min.* **20,** 368 (1983).
40. J. M. REAU, A. RHANDOUR, C. LUCAT, J. PORTIER, AND P. HAGENMULLER, *Mater. Res. Bull.* **13,** 827 (1978).
41. P. DARBON, J. M. REAU, P. HAGENMULLER, C. DEPIERREFIXE, J. P. LAVAL, AND B. FRIT, *Mater. Res. Bull.* **16,** 389 (1981).
42. J. M. REAU, S. MATAR, S. KACIM, J. C. CHAMPARNAUD-MESJARD, AND B. FRIT, *Solid State Ionics* **7,** 165 (1982).
43. S. KACIM, J. C. CHAMPARNAUD-MESJARD, AND B. FRIT, *Rev. Chim. Miner.* **19,** 199 (1982).